Measurement of freezing point depression of water in glass capillaries and the associated ice front shape

Zhihong Liu,[1] Ken Muldrew,[2,*] Richard G. Wan,[1] and Janet A. W. Elliott[3]
[1]*Department of Civil Engineering, University of Calgary, Calgary, Alberta, Canada T2N 1N4*
[2]*Department of Cell Biology and Anatomy, University of Calgary, Calgary, Alberta, Canada T2N 4N1*
[3]*Department of Chemical and Materials Engineering, University of Alberta, Edmonton, Alberta, Canada T6G 2G6*
(Received 28 October 2002; published 16 June 2003)

Variations of the Kelvin equation [W. Thomson, Philos. Mag. **42**, 448 (1871)] to describe the freezing point depression of water in capillaries exist in the literature. The differing equations, coupled with the uncertainty in input parameters, lead to various predictions. The difference between the predictions may become substantial when the capillary size decreases much below micron dimensions. An experiment was designed to investigate the predicted values using a customized directional solidification stage. The capillary freezing point depression for glass tubes with radii of 87 μm–3 μm was successfully measured. The image of the ice-water interface at equilibrium was also digitally captured and analyzed to examine the contact angle and the interface shape as well. Both are important for examining the hemispherical interface assumption that was exclusively used in the theoretical derivations. Finally, an equilibrium analysis of the thermodynamic system leads to a theoretical discussion of the problem. The effect of the temperature gradient on the interface shape is addressed, and an engineering criterion for the critical temperature gradient above which the effect must be considered for the interface shape calculation is derived.

DOI: 10.1103/PhysRevE.67.061602 PACS number(s): 68.08.−p, 68.37.−d, 82.65.+r, 87.16.Dg

I. INTRODUCTION

The interface of an ice crystal in a glass microcapillary is highly curved and forms a contact angle with the capillary wall which depends upon the interfacial excess energies between the solid, liquid, and wall (Fig. 1). The temperature at which the crystal is thermodynamically stable is also a function of the capillary diameter. As the diameter decreases, the freezing point of water is lowered, which is called the capillary freezing point depression. The relation between the freezing point depression and the curvature of the interface is described by the Kelvin equation [1]. The original Kelvin equation was a liquid-vapor version that quantifies the deviation in equilibrium vapor pressure above a curved surface from that which would exist above a plane surface at the same temperature. It was later extended to solid-liquid phases and became well known as the ''Gibbs-Thomson'' relation in solidification that defines the local displacement of equilibrium temperature on a curved solid-liquid interface [2,3]. According to this relation, the freezing point depression due to curvature is

$$\Delta T = T_C - T_E = -\frac{\nu_S \sigma_{\mathrm{LS}} T_E}{L}\kappa, \tag{1}$$

where κ is the mean curvature of the interface (m^{-1}), ν_S is the specific volume of the solid phase (m^3/kg), L is the latent heat of fusion (J/kg), σ_{LS} is the interfacial excess energy per unit area of ice-water interface ($\mathrm{J/m}^2$), and T_C and T_E are the freezing point and the normal equilibrium temperature of the ice-water interface (i.e., 273.15 K), respectively.

Based on a direct variational analysis of the system free energy, Jackson and Chalmers (1958) derived the critical temperature T_C, below which a solid interface will propagate along a capillary [4]. Assuming the radius of the capillary is r, the freezing point depression was given by

$$\Delta T = \frac{\sigma_{\mathrm{LS}} T_E \cos\alpha}{lr}, \tag{2}$$

where $l = \rho_S L$ is the latent heat of fusion per unit volume of ice ($\mathrm{J/m}^3$) and ρ_S is the density of ice. The equilibrium contact angle α between the solid-liquid interface and the capillary wall was determined by the Young equation

$$\sigma_{\mathrm{LB}} = \sigma_{\mathrm{SB}} + \sigma_{\mathrm{LS}} \cos\alpha, \tag{3}$$

where σ_{LB} and σ_{SB} are the interfacial tensions for the liquid-wall and solid-wall interfaces, respectively.

This problem was revisited by Mazur (1966) in order to understand how the cell membrane acts as an effective barrier to ice nucleation or seeding at supercooled temperatures of $-5\,^{\circ}\mathrm{C}$ to $-13\,^{\circ}\mathrm{C}$ [5]. An estimate of the critical temperature supports his hypothesis that intracellular ice is nucleated

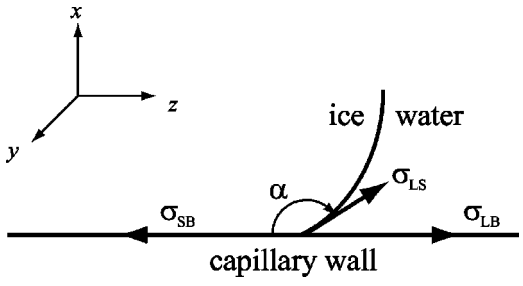

FIG. 1. An ice front in a capillary with a contact angle.

*Corresponding author. Email address: kmuldrew@ucalgary.ca

TABLE I. Diverse values given in the literature for the freezing point of water in glass capillaries.

α	r (μm)	$\lvert\Delta T\rvert$ (K)	Γ (K μm)	Source
180° (assumed)	5	0.0057	0.0285	Eq. (2) [4]
180° (assumed)	5	0.0102	0.0512	Eq. (4) [5]
180° (assumed)	5	0.0114	0.0569	Eq. (5) [9]

by the growth of extracellular ice through the aqueous pores (radii 0.3–0.85 nm) of the cell membrane. Even today, the mechanism of intracellular ice formation (IIF) remains unsettled and is a central topic in cryobiology [6–9]. Through a different procedure from that of Ref. [4] (details will be reviewed later in the section entitled ''equilibrium analysis''), Mazur [5] obtained

$$\Delta T = \frac{2\nu_L \sigma_{\mathrm{LS}} T_E \cos\alpha}{Lr}, \tag{4}$$

where ν_L is the specific volume of water (note that in Mazur's derivation he assumed $\nu_S \approx \nu_L$). Also, in Eq. (4), the curvature has been replaced by $2\cos\alpha/r$ when compared with the Gibbs-Thomson equation, Eq. (1). Mazur was the first person to relate the freezing point in a biological capillary to the Kelvin equation. The correct coefficient ''2'' was also introduced in the right hand side of his equation, as compared with Eq. (2).

Recently, Acker *et al.* (2001) proposed a theoretical derivation for the equilibrium of ice with an *aqueous* solution in a capillary [9]. The major advance they made was to derive the total freezing point depression in two superposition terms: one from the capillary effect and another from the osmotic effect; i.e.,

$$\Delta T = \frac{2\nu_S \sigma_{\mathrm{LS}} T_E \cos\alpha}{Lr} + \frac{\nu_L \pi_L T_E}{L}, \tag{5}$$

where π_L is the osmotic pressure of the solution. Without considering the osmotic term, Eqs. (5) and (4) differ by 10% due to using different specific volumes ν_S and ν_L. Table I compares the three theoretical predictions for a capillary radius of 5 μm. Note that in Table I, we have assumed that $l = 3.07\times10^8$ J/m^3, $\sigma_{\mathrm{LS}} = 3.2\times10^{-2}$ N/m [10]. For the convenience of comparison, a ''capillarity coefficient,'' $\Gamma = \lvert\Delta T\rvert r/\cos\alpha$, has been defined.

Until this work, there had been no direct experimental verification of the capillary freezing point depression, attributable to the difficulty in determining the required interfacial tension and contact angle independently. Indirect experiments, however, with freezing liquids that were confined in mesoporous materials, have been performed by measuring the nuclear magnetic resonance or x-ray signals as a function of temperature. The pore size of the porous materials examined ranges from 6–100 nm [11], 2–3 nm [12], and 1.2–2.9 nm [13]. The results strongly support the Kelvin equation, in that the freezing point depression measured can be related to the reciprocal of the pore radius with a simple linear function. The proportional constant for this linear function (i.e., the product of Γ and $\cos\alpha$) was found to lie between 0.0495 K μm and 0.0676 K μm [12,13]. Recent experiments of ice growth through cell gap junctions (with a pore radius of 0.75 nm) [9] also suggest that the Kelvin equation is at least qualitatively consistent with the temperature-dependent phenomenon of intracellular ice propagation.

As listed in Table I, for a 5 μm (radius) capillary, the difference in the predicted ΔT is less than 0.006 K. However, the predicted freezing points will diverge appreciably as the capillary size goes down to the scale of biological pores. For instance, the difference can become as much as 33 K for the aqueous pores in the cell membrane. Even worse, the predicted values also suffer from the uncertainty in the contact angle α [5,9]. For these reasons, we were led to look for a direct experimental verification of the Kelvin equation to determine the interfacial tension and/or the contact angle, separately. This is applicable not only to the theories of IIF, but also a necessary step for further applications in the freezing of porous and/or biological tissue systems. Freezing point depression is also responsible for ''frost heave'' and ''ice lensing'' in porous systems such as soils [4,14]. On the other hand, cryopreservation of cells, tissues, and organs for use in transplantation has been limited to cell suspensions and several simple tissue systems. One of the primary obstacles is that the freezing mechanisms in tissues are not yet well understood [15,16]. In a recent SEM study of frozen articular cartilage, Muldrew *et al.* [17] hypothesized that the mechanism behind the extensive cryoinjury could be very much similar to that of ice growth in a capillary-porous medium, in that the tissue matrix may function like a ''porous'' structure that changes the patterns of ice formation and solute diffusion inside, resulting in dramatically altered ice morphology.

In this paper, we placed fine glass capillary tubes filled with water or aqueous solutions across a prescribed temperature gradient via a directional solidification cryostage. Once the capillaries reached a thermal steady state, ice was seeded by touching dry ice to the capillaries. The location of the equilibrium interface was then measured under a microscope to find the corresponding equilibrium temperature. To improve the accuracy of measurement, a customized cryostage that offers a shallow temperature gradient as low as 10^{-5} K/μm has been developed [18].

To our knowledge, there has not previously been a direct measurement of the shape of a solid-liquid interface in a capillary small enough to be significantly affected by the Kelvin effect. As a result, an equilibrium contact angle and a spherical ice front have been exclusively assumed in all theoretical models to use the Laplace equation (the Laplace equation relates the local pressure drop across the interface due to the surface tension with the curvature of the interface). These assumptions were examined in the second part of the experiment by recording the interface image with a digital camera to observe the interface shape and the contact angle as well. In previous related experimental tests (see, e.g., Refs. [9,10]), the contact angle and/or the solid-liquid interfacial tension were left as fitting parameters. A major advance that has been made in the present paper work is the parallax calculation of the light path that is distorted by the

cylindrical wall of the glass capillaries. It can be shown that for an equilibrium state in a uniform temperature system, if it exists, the interface forms a hemisphere.

The necessary conditions for thermodynamic equilibrium of the capillary system are discussed in the section called ''equilibrium analysis.'' It will be shown that the combination of the Kelvin equation and the Young equation gives a complete description of the problem considered, including the interface shape. Therefore, it seems more reasonable to treat the spherical interface as a specific condition of equilibrium under a particular circumstance, rather than a general assumption to be used in the theoretical derivations.

The effect of the temperature gradient on the interface shape is also briefly discussed and an engineering criterion is given for the critical temperature gradient G^*, above which the gradient will have an influence on the interface shape.

II. EXPERIMENTAL APPARATUS

The experiment reported, herein, used ice growth in fine glass capillaries across a constant temperature gradient, which was supplied by a directional solidification cryomicroscope. A directional solidification cryomicroscope utilizes a stage with a fixed spatial temperature gradient through which the specimen is mounted or moved in time to produce the desired thermal history [19]. It consists of two separated copper bases and one bridging plate (usually a glass microscope slide). The bases are maintained at two different but constant temperatures.

Because of its exposure to the ambient air, the slide does not always supply a linear temperature profile in its longitudinal direction. Based on a 1D thermal conduction analysis, a criterion for linear thermal profile design is to keep the parameter

$$\psi = d\sqrt{\frac{2h}{tk_{\text{slide}}}} < 0.3, \tag{6}$$

where t is the thickness of the slide, d is the separating distance between the two copper bases, h is the heat transfer coefficient of the slide, and k_{slide} is its thermal conductivity. For a 0.5-mm-thick glass slide, the maximum separating distance satisfying Eq. (6) is 3.219 mm [20]. This is the maximum allowable span for a glass slide to supply a linear temperature profile. In our experiment, we developed a cryostage using a sapphire slide of $60\times25\times1$ mm^3 (Almaz Optics, Inc., NJ, US) as the bridging substrate [18]. The sapphire slide offers a wider separating distance ($d=10$ mm), a lower temperature gradient, and more importantly, a more linear profile between the two blocks, due to its higher thermal conductivity (27 times of that of a glass slide).

Two $25\times25\times3.1$ mm^3 thermoelectric (TE) modules (CP0.8-127-05L, Melcor Corp., NJ, US) were sandwiched between the copper bases and two additional copper plates, respectively, as shown in Fig. 2. The TE units used the Peltier effect and worked as ''heat pumps.'' The plates, which were placed on the top of TE modules, were made thin and small in mass so as to generate a fast cooling rate. Each plate contained a thermocouple (5TC-TT-T-30, Omega Engineering, Inc., CT, US) inside for temperature monitoring. The copper bases were connected to an ice-water bath through a utility pump (Little Giant Pump Co., OK, US), to remove the dissipated heat. The copper bases and plates were enclosed within an acrylic box for heat insulation and represented a compact cryostage.

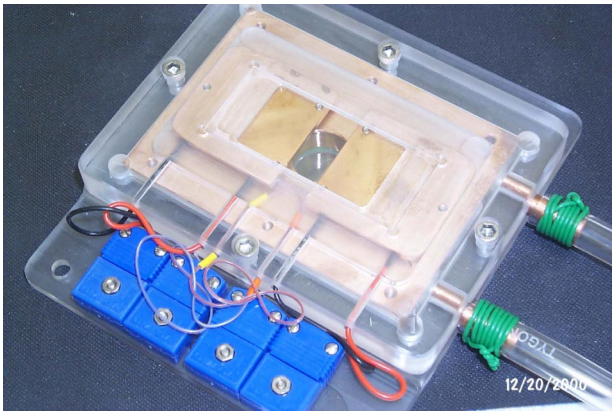

FIG. 2. A temperature gradient stage with two thermoelectric modules and one sapphire slide.

Two independent control systems (PI, 2000 Hz) were used for controlling both the higher and the lower temperatures through the TE modules. This was done via configuration of a conventional dual loop temperature control unit (The GCC Company, AB, Canada) as well as customized temperature profile software. Using the sapphire slide, the TE stage can offer a temperature gradient as low as 10^{-5} K/μm. The maximum cooling rate is 300 °C/min and the working range is between -20 °C and $+20$ °C, if ice water is used as a coolant. The higher and lower temperature profiles were recorded once per 0.1 sec, as shown in Fig. 3.

Local temperatures along the longitudinal axis of the slide were measured with a moving ring that contained a thermo-

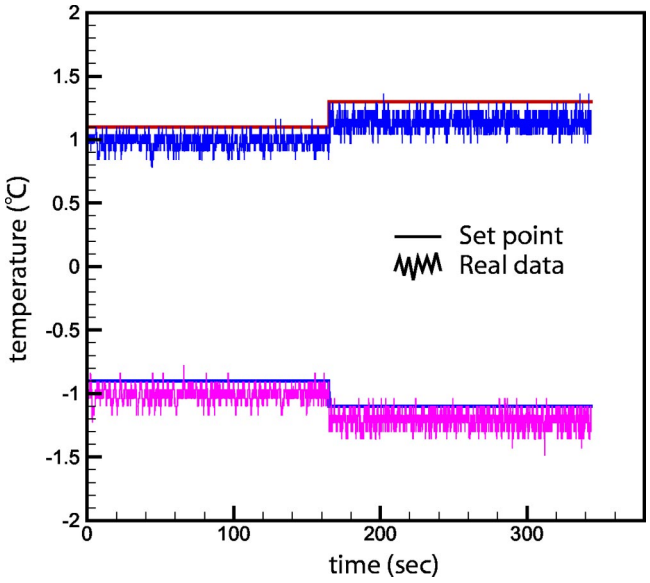

FIG. 3. Temperature profiles with time produced by the TE cryostage.

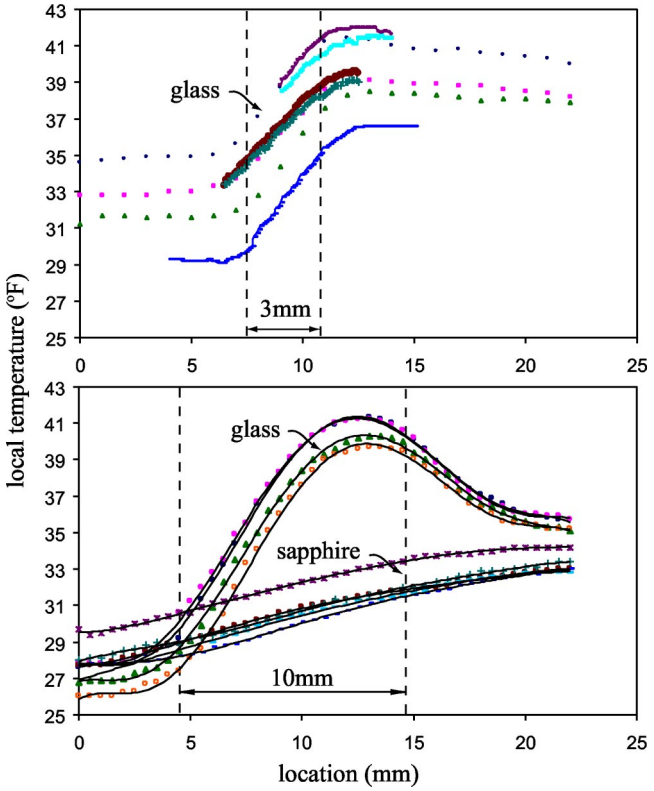

FIG. 4. The measured temperature profiles for glass and sapphire slides (data were obtained on various dates).

couple (C02-T 0.0005 in., Omega Engineering, Inc., CT, US). The ring sandwiched the thermocouple between two 18-mm circular cover glasses (Fisher Scientific, Canada) with epoxy (Omegabond 100, Omega Engineering, Inc., CT, US). Then, the ring was attached to a 10-mm vinyl tubing (TYGON 5/8- in.-ID) that just fitted the microscopic objective lens (Zeiss, Germany) to obtain a close but soft connection. Focusing of the lens also supplied a pressure to maintain a good contact between the thermal measuring device and the sapphire top surface. A microprocessor based thermometer (HH23, Omega Engineering, Inc, CT, US) read the temperature. Two gaps, 3 mm and 10 mm, were examined for glass and sapphire slides, respectively. The temperature profiles measured on various dates are shown in Fig. 4, in which the unit °F (rather than °C) was used for better resolution. Clearly, the sapphire slide can give a reasonably linear temperature profile over the span of 10 mm.

Additional solidification experiments with solution-filled glass pipettes (1 μL, Drummond Scientific Company, PA, US) were performed. The location of ice fronts for various aqueous solutions was plotted against the osmolality measured by a standard Osmometer (Precision Systems Inc., MA, US). A perfect linear correspondence was obtained (data not shown), which indicates the capability of the new cryostage. Potassium permanganate (Sigma Chemical Co., MO, US) was used for making aqueous solutions. A Pixera 120es digital camera with a resolution of 1260×960 pixels (Pixera Corporation, CA, US) was used for recording front images for the ice structure analysis.

III. MEASUREMENT OF FREEZING POINT DEPRESSION

Fine capillaries were fabricated by heating the middle portion of a micropipette (5 μL, Fisher Scientific, Canada) as evenly as possible over a gas burner by rotating until it started to soften; then the micropipette was removed from the flame and immediately drawn by hand in a free space. Generally, the quicker the pipette is drawn, the finer the capillary. It is not too difficult to get down to 6 μm (ID) using this method. Before drawing capillaries, the micropipette has to be carefully cleaned to remove any oil or dust inside, since a dirty glass wall may give a misleading contact angle or position of equilibrium. The cleaning procedure used was as follows: (1) Connect the micropipette to a 10 cc syringe (Becton Dickinson and Company, NJ, US) and wash inside back and forth with tap water; (2) soak the micropipette in chromic acid (10 wt. %, Fisher Scientific, Canada) overnight; (3) rinse the tube with room temperature distilled water (Millipore) thoroughly for ≈5 min; (4) rinse with hot distilled water (place water bottle in hot boiling water for 5 min and use this water to rinse the tube); and (5) let the tube dry in air (nondusty environment).

Measurement of freezing point depression was correlated to the distance between a planar ice front and a curved one produced *simultaneously* under the *same* temperature field conditions, rather than a thermocouple reading that is subject to thermal fluctuations or environmental noises. Basically, two fine glass capillaries, of the same or similar diameters, were immersed and placed in parallel into a drop of distilled water (about 4 μL) that was sandwiched between the sapphire slide and a 12-mm circular glass cover slip. The drop of water became the bulk water in which a planar ice front would form and used as base line. One of the glass capillaries was filled with a dilute aqueous solution, instead of water. Therefore, besides capillary depression, the solution in this glass capillary was also subjected to a constitutional freezing point depression due to concentration [the osmotic term in Eq. (5)]. This made the location of the ice front shift further away from the bulk ice front and from the ice front in the capillary containing pure water. Comparing the distances between these fronts, the component of freezing point depression due to the capillary effect was deduced knowing the location of the front produced in the solution. In this sense, the osmolality of the solution worked like an "*in situ*" thermometer that measures the capillary depression in the manner of an osmometer. The freezing protocol used in the experiments is as follows.

(1) Let both sides of the stage cool down to −15 °C and hold. Initiate freezing, both inside and outside of the capillaries, with dry ice.

(2) Warm up both blocks, slowly, to reach a desired temperature gradient (e.g., −4 °C and +1 °C at the two blocks, respectively). Microadjust the gradient to make sure all the ice fronts are sitting within the view of the microscope.

(3) Allow time for solute to diffuse away from the ice front if there are aqueous solutions involved. It normally takes about 15–30 min.

(4) Record the image for later analysis with the digital camera.

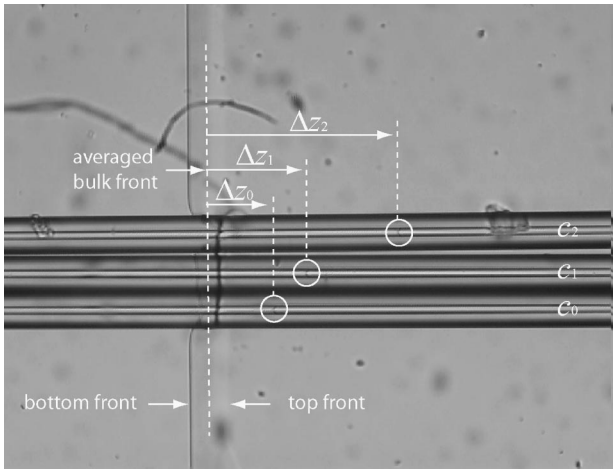

FIG. 5. Ice fronts under the microscope. Three curved fronts are marked with circles, corresponding to concentrations of 0, 8, and 16 mOsm, respectively. The longest dashed line is the averaged bulk front.

(5) Stop freezing and wait for thaw. Put suspensions of certified latex beads (10 or 20 μm diameter, Coulter Electronics, Inc., FL, US) into the bulk water. Take a snapshot that will be used for the calibration of the image software (Pixera Studio Pro, Pixera Corporation, CA, US) and for the determination of the average diameter of the capillaries as well as the distances in the images.

Multiple capillaries were used in a test group to ensure accuracy (see Fig. 5). Two bulk ice fronts were usually seen in a microscope view: one was a dark line at the bottom of the water layer; another was light, and not too obvious, at the top. The two lines were due to a small temperature difference along the thickness (less than 8×10^{-5} K/μm). For this reason, the midpoint between these two fronts, i.e., the averaged bulk front was used for the distance measurement. According to Eq. (5), the total freezing point depression in a capillary is written as

$$\Delta T_i = G\Delta z_i = -\beta c_i + \Delta T_C, \tag{7}$$

where ΔT_C is the capillary depression; G is the transient temperature gradient of the stage; Δz_i is the distance from the averaged planar ice front (which has already been assumed to correspond to the equilibrium temperature T_E); β is the freezing point constant, $\beta = 1.86$ K/(mol/kg) for dilute aqueous solutions [21]; and c_i is the osmolality of the solutions. The above equation is then rewritten as

$$\beta c_i = -G\Delta z_i + \Delta T_C. \tag{8}$$

Thus, if we plot the absolute values of the osmotic freezing points of the solutions, βc_i, against the displacement from the bulk front to its own curved one, Δz_i, and fit the data with a linear extrapolation, we immediately obtain the capillary depression ΔT_C by finding its intercept with the vertical axis. The value of the transient temperature gradient of the cryostage G can also be estimated from the slope of this extrapolation line.

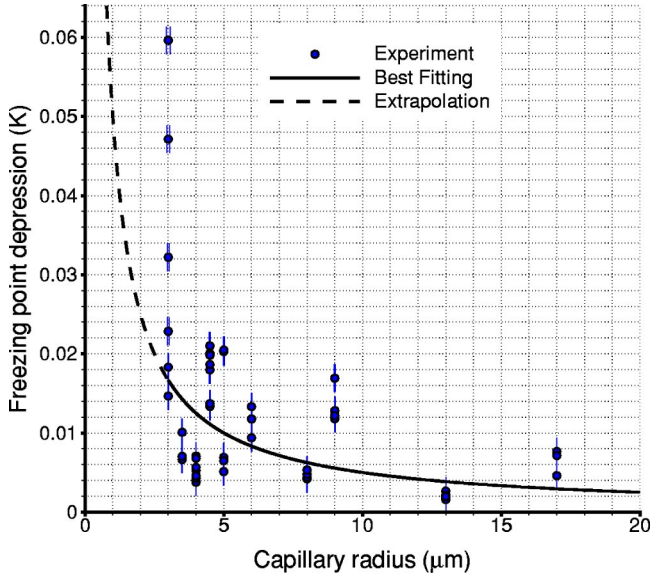

FIG. 6. Freezing point depression vs the capillary radius. The experimental data are fitted with an inversely proportional curve.

More than 140 digital images were collected over a period of several months and analyzed using this method. The measured capillary freezing point was associated with the averaged capillary inner diameter of a sampling group. For example, a freezing point depression of 0.01 K was found for a capillary radius $r = 5$ μm, as shown in Fig. 6. The best hyperbolic approximation to the experimental data is

$$\Delta T = -\frac{0.050 \text{ K } \mu\text{m}}{r} \tag{9}$$

with a regression coefficient of 0.37. Note that the data points at $r = 3$ μm were not used in the fitting due to their scatter. It is also cautioned here that, due to the lack of data for capillary radii less than 3 μm, the proposed fit only gives a trend on the freezing point depression within that particular

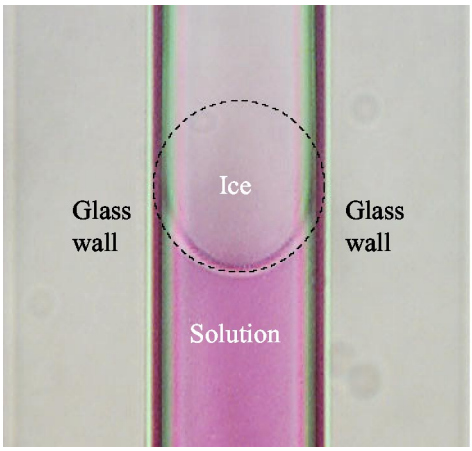

FIG. 7. An ice front in a 20-μm ID glass capillary. The interface is distorted by the capillary wall. The dashed circle is for comparison. The solution below the interface is potassium permanganate.

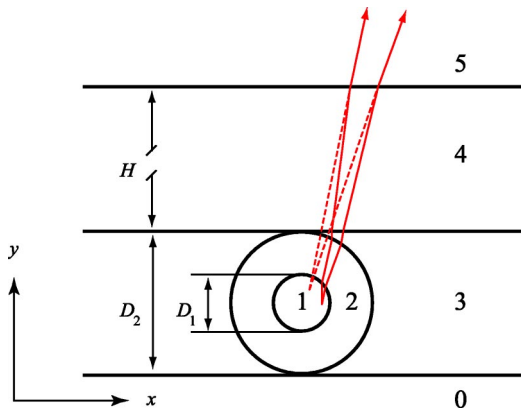

FIG. 8. The schematic configuration for the light path calculation. Various media are numbered.

range. This has to be further investigated in future as the technique of fabricating submicron capillaries becomes mature.

IV. MEASUREMENT OF INTERFACE SHAPE

Shown in Fig. 7 is an image of an ice front (top view) created in a liquid potassium permanganate solution within a 20-μm ID glass capillary. Four of the pictures taken at intervals were selected and summarized for image analysis. Although it appears superficially that the best fit for the interface is *not* a half circle, this does not mean that the hemispherical interface assumption used in the theoretical derivations is not correct, since the light path is distorted when passing through the curved capillary wall, especially when the capillary diameter is small.

The refraction of light can be calculated according to Snell's law (see, e.g., Ref. [22]). Assuming that light travels from a material with refractive index n_1 into a material with refractive index n_2, the refracted ray, the incident ray, and the normal to the surface should all lie in the same plane and the angle of refraction α_2 is related to the angle of incidence α_1 by

$$n_1 \sin \alpha_1 = n_2 \sin \alpha_2 . \tag{10}$$

For a cylindrical interface, the unit radius was chosen as the normal. Given the coordinates of the objective and the geometric configuration that the light will pass through (such as that shown in Fig. 8), we are able to extend the light path and find one by one the points of incidence on medium interfaces.

A numerical algorithm was developed and implemented into a computer program. First, the prescribed geometry of the interface (for example, one half of a circle in a horizontal plane) was subdivided evenly into 100 linear ''elements,'' each of them having two ''nodes.'' The nodes are the joints between elements. Second, we let each node on the interface emit at least two rays of light, one vertically upward (y direction) and another having a small angle (about 0.01°) to the vertical line, but still remaining in the x-y plane. Both rays went through all the optical media: the solution (or water), the glass capillary wall, the bulk ice, the cover slip, and the air (as numbered from ''1'' to ''5'' in Fig. 8), until they reached the microscope. The final light paths at medium ''5'' were reversed to find the crossing point. This point should be the virtual ''node'' that we normally observe under a microscope. Connecting these virtual ''nodes'' by linear elements will give the ''distorted'' image of the objective. Table II gives a list of parameters used in the calculation.

TABLE II. Parameters used for calculation: (I) for calibration; (II) for measurement of interface.

	Code	Note	I	II
Refraction	0	Sapphire (slide)	1.77	1.77
Index	1	Water/solution	1.33	1.33
	2	Glass (capillary)	1.50	1.50
	3	Oil (immersion)/ice (bulk)	1.51	1.31
	4	Glass (cover slip)	1.50	1.50
	5	Oil/air	1.51	1.00
Dimensions	D_1	Inner diameter	16	20
(μm)	D_2	Outer diameter	81	88
	H	Thickness (cover slip)	170	170

The computer program was calibrated by comparing the predicted and the observed images of a standard spherical bead (10 μm diameter, Coulter Electronics, Inc., FL, US). The bead was placed within a 16-μm ID capillary, which was sandwiched with immersion oil ($n=1.51$, Zeiss, Germany) between the sapphire slide and a 170-μm-thick cover slip. Immersion oil also filled the gap between the cover slip and the microscope lens. As shown in Fig. 9, the width of the measured ''sphere'' was shortened in the microscopic image to about 86% of its longitudinal value. This is very close to the predicted value of 88% based on the numerical calculation.

Assuming the original interface is a hemisphere with a radius of r, and taking account of the material parameters and the configuration geometry of the optical media in the computer program, we arrive at the distorted ''circle'' that is shown as a solid line in Fig. 10. This distorted ''circle''

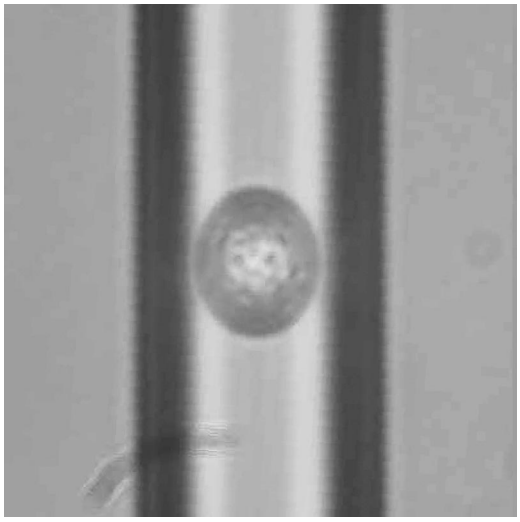

FIG. 9. A standard bead (10 μm diameter) within a capillary.

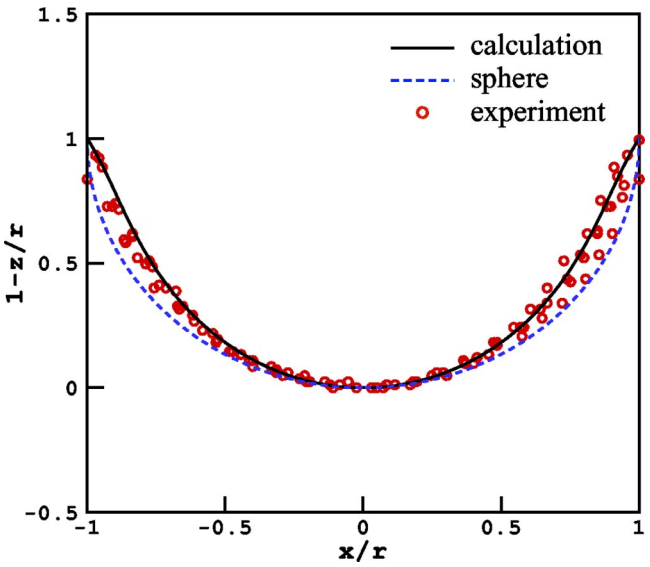

FIG. 10. A distorted "sphere," calculated from the program, matches the experimental data.

matches the experimental data quite well. Thus, we conclude that within the experimental error, the interface within the capillary is a perfect hemisphere and the contact angle is 180°.

V. EQUILIBRIUM ANALYSIS

As emphasized in a recent paper [23], three conditions are required for the equilibrium of a thermodynamic system that contains a line of contact between solid and liquid phases in a capillary with an ideal wall surface: (1) the Young equation; (2) the Laplace equation; and (3) a condition on the chemical potentials of the components. These conditions were originally derived by Gibbs [24], based on a variational analysis. To be equivalent to the variational criteria, the three equilibrium equations have to be satisfied *simultaneously* to define a thermodynamic equilibrium state.

For a system without a gravitational interaction, combination of the Laplace equation and the relation of chemical potential equality will lead to the Kelvin equation [25]. The Kelvin equation together with the Young equation, therefore, completely describe the equilibrium state, including the freezing point, interface shape, and contact angle in capillaries. The derivations of Mazur [5] and Acker *et al.* [9] basically followed this theoretical line. The Jackson and Chalmers' equation was based on a direct variational analysis [4]. Unfortunately, their variational function was not complete and their formulation can be improved to yield the correct answers.

In a uniform temperature field, the interface is isothermal and the solute concentration near the interface is also constant. In this specific circumstance, the Kelvin equation directly yields the interface being a part of sphere. The Young equation then relates the interface curvature with the capillary radius through the contact angle; i.e.,

$$-\frac{\kappa}{2/r}=\cos\alpha=\frac{\sigma_{\mathrm{LB}}-\sigma_{\mathrm{SB}}}{\sigma_{\mathrm{LS}}}. \tag{11}$$

Only certain combinations of the physical parameters of σ_{LS}, σ_{SB}, and σ_{LB} will give a stable contact angle [26]. If the contact angle is 180°, then the interface is a hemisphere with a mean curvature of $2/r$ and the freezing point depression is

$$\Delta T=-\frac{2\nu_S\sigma_{\mathrm{LS}}T_E}{Lr}. \tag{12}$$

The solid-liquid interface, in general, is not a hemisphere. For example, for an interface across a temperature gradient, the interface curvature will be modified in response to the temperature difference within the ice front. Ignoring the effects of any solute concentration gradients, the deviation of the interface from spherical can be estimated according to the Kelvin equation by comparing the difference between the two situations of zero and constant temperature gradients.

Let G be the constant temperature gradient ($G>0$). The local freezing point of the interface, in a stable state, should be equal to the externally applied temperature on the stage; i.e.,

$$T_E-\frac{\nu_S\sigma_{\mathrm{LS}}T_E}{L}\kappa(z)=T_{\mathrm{Ref}}+Gz, \tag{13}$$

where T_{Ref} is a *reference temperature* that is chosen in the field for the convenience of calculation and z is the distance from this reference point, positive in the ice growth direction.

For the case of zero temperature gradient, since the interfacial freezing point is a constant (i.e., T_C) in the uniform temperature field ($G=0$) and $\kappa(z)\equiv 2/r$, if the contact angle is assumed to be 180°, as discussed before, one has

$$T_E-\frac{\nu_S\sigma_{\mathrm{LS}}T_E}{L}\frac{2}{r}=T_C=T_{\mathrm{Ref}}, \tag{14}$$

which requires that the common reference temperature T_{Ref} for various temperature gradients be the capillary freezing point T_C, which is also the local freezing point on the contact line of the liquid, solid, and wall. Subtracting Eq. (14) from Eq. (13) leads to

$$-\frac{\nu_S\sigma_{\mathrm{LS}}T_E}{L}\left(\kappa-\frac{2}{r}\right)=G\,z, \tag{15}$$

in which $0<z<r$. This equation will yield the interface shape in a temperature gradient (Fig. 11; see the Appendix for the solution procedure).

It also becomes apparent that if

$$G\ll G^*=-\frac{\Delta T}{r}=\frac{2\nu_S\sigma_{\mathrm{LS}}T_E}{Lr^2}<\frac{2\nu_S\sigma_{\mathrm{LS}}T_E}{Lrz}, \tag{16}$$

then the curvature deviation is small; i.e.,

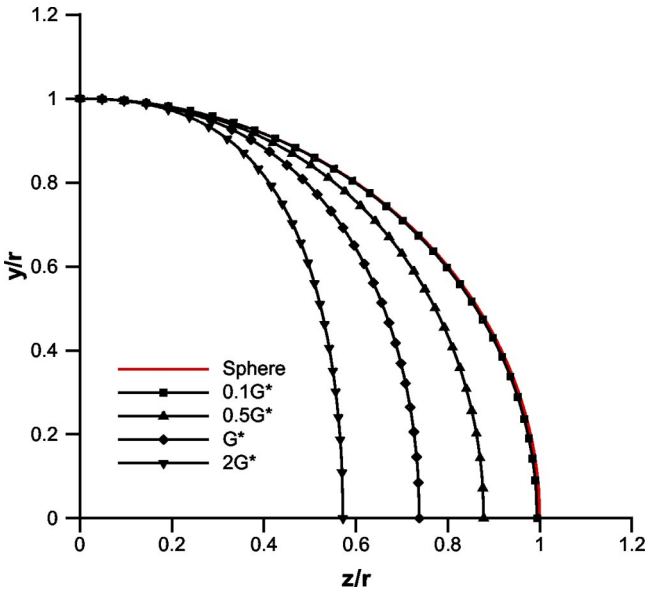

FIG. 11. Ice fronts in temperature gradients (G^* is the critical temperature gradient).

$$\left|\kappa-\frac{2}{r}\right| \Big/ \left(\frac{2}{r}\right) \ll 1, \tag{17}$$

which implies that the interface is still close to spherical. Here G^* is defined as the *critical temperature gradient*. For example, if $r=10$ μm, then $G^* \approx 6\times 10^{-4}$ K/μm. That is to say for any temperature gradient less than 6×10^{-5} K/μm (one order of magnitude smaller than G^*), there will be little deviation of the interface from a hemisphere. This has been examined in our experimental measurement of the interface shape in a shallow temperature gradient (about 2×10^{-5} K/μm), which is very close to a hemisphere. If the temperature gradient $G \geqslant G^*$, then the interface will be affected. Details of the temperature gradient effect on the interface shape will be discussed in a separate paper.

VI. CONCLUSION AND DISCUSSION

An experiment has been designed to measure the freezing point depression of water in glass capillaries. The capillarity coefficient (Γ) was first separated from the combined effects with the contact angle and was experimentally found to be 0.050 K μm for the glass tubes with radii of 87 μm–3 μm. This value is close to the theoretical predictions based on Eqs. (5) and (4), and also consistent with the measurements at nanometer scales [12,13], assuming that the contact angles were 180° in their experiments. While the experiments presented herein are the first of their kind, they are not yet accurate enough to distinguish, for example, between Eqs. (5) and (4) which differ by 10%. Although it was clear to the authors of both Eqs. (4) and (5) that Eq. (5) with ν_S instead of ν_L was the correct form, it would be nice to experimentally verify Eq. (5) with more precision in the future.

Assumptions on the spherical shape and the contact angle have been verified in the present study as well. In contrast to previous experimental investigations of the Kelvin equation, our experiment can verify the theoretical equations, the contact angle, and the interface shape, separately. Digital image analysis supports the conclusion that the equilibrium interface in a glass capillary in a shallow temperature gradient is very close to a hemisphere, with a contact angle of almost 180°. Therefore, the spherical interface assumption used in earlier derivations is valid, especially for capillaries with smaller radii, since the critical temperature gradient is inversely proportional to r^2. The interface will not be a hemisphere in a capillary in a large temperature gradient.

Although there is no direct way to measure the interfacial excess energy of an ice-water boundary, σ_{LS}, it has been estimated by several indirect methods. Fletcher (1962) concluded that it probably lies between 10 and 25 ergs/cm^2 for the ice-pure water interface, with the most likely values being 17 ergs/cm^2 near $-40\,^\circ$C and about 20 ergs/cm^2 near 0 °C [27]. A more recent measurement is 32 ergs/cm^2 [10]. Our experimental data support this value. In addition, the procedure developed in the present paper can be extended and modified to estimate the interfacial tension of the ice-*solution* (not ice-water) interface based on Eq. (5).

Of course, care must be taken when using the capillary freezing point depression equation for very small radii, though the liquid-vapor Kelvin equation has been verified down to 4 nm [28]. With decreasing diameter, there may be significant deviations in the microscopic interactions of water and the pore as we approach molecular dimensions. The specific entropy of ice may also become temperature dependent at lower temperatures. Molecular dynamics simulation of freezing in nanopores indicates that the resulting ice is a crystal bilayer that does not resemble any ice found so far [29]. Nevertheless, the experiments with mesoporous materials suggested that the Kelvin equation can still be used in the nanometer range by introducing the ''effective'' capillary radius [12], which is the capillary radius minus the thickness of the so-called ''bound water.'' The bound water refers to the unfrozen part of water adjacent to the pore wall [13]. The exact thickness of the bound water has not yet been established, though an assumption of bimolecular thickness has been used [13].

The contact angle of an ice front in a biological pore, such as a blood vessel, is assumed to be much less than 180° and may well approach 90° [5]. This can be verified by a similar experiment. The primary idea is to put a coating layer of polymer that is similar to a lipid membrane on the inner wall of a glass capillary so that the wall property is changed. Future work based on the same procedure as developed in the present paper can help us understand more about the freezing of biological tissues.

The apparatus developed in the present paper will also be amenable to studying the kinetic effects such as diffusion-limited ice growth in tissue freezing [17]. Details will be discussed in a future paper.

ACKNOWLEDGMENTS

This work was supported by the Whitaker Foundation and NSERC (Natural Sciences and Engineering Research Coun-

cil of Canada). This research was supported by the Canada Research Chairs Program. The authors would like to express their sincere thanks to Sherri Liang, May Chung, Simon Chi, Colleen Chan, Dr. Ayodeji Jeje, and Dr. John Matyas for their discussions and technical assistance.

APPENDIX: THE INTERFACE SHAPE IN A TEMPERATURE GRADIENT

Assuming the interface is a general surface of revolution, one has

$$\varphi(x,y,z)=x^2+y^2-R^2=0, \tag{A1}$$

where $R=R(z)$ is the interface outline and z is the growth direction of the ice front. The surface mean curvature is obtained following a level set approach [30]; i.e.,

$$\kappa=\mathrm{div}\left(\frac{\nabla\varphi}{\sqrt{\nabla\varphi\cdot\nabla\varphi}}\right)=\frac{R^2[1-(RR')']+2(RR')^2}{[R^2+(RR')^2]^{3/2}}, \tag{A2}$$

where ∇ is the gradient operator and $R'=dR/dz$. The governing equation for the interface shape is

$$-\frac{v_S\sigma_{\mathrm{LS}}T_E}{L}\left(\kappa-\frac{2}{r}\right)=G\,z, \tag{A3}$$

where G is the temperature gradient. To find a numerical solution, the interface shape can be approximated by a polynomial series following Pascal's triangle. Having considered the boundary conditions at the capillary wall and terminated the polynomials at a bicubic order, the interface equation can be rewritten as

$$\frac{R^2}{r^2}=1+\frac{a_2\dfrac{z^2}{r^2}+a_3\dfrac{z^3}{r^3}}{1+a_1\dfrac{z}{r}} \tag{A4}$$

and

$$\frac{RR'}{r^2}=\frac{1}{2r}\,\frac{2a_2\dfrac{z}{r}+(3a_3+a_1a_2)\dfrac{z^2}{r^2}+2a_1a_3\dfrac{z^3}{r^3}}{\left(1+a_1\dfrac{z}{r}\right)^2}. \tag{A5}$$

Substituting Eqs. (A4) and (A5) into Eqs. (A2) and (A3), the unknown coefficients a_1, a_2, and a_3 can be found by a regression iteration.

[1] W. Thomson, Philos. Mag. **42**, 448 (1871).
[2] D.P. Woodruff, *The Solid-Liquid Interface* (Cambridge University Press, London, 1973), p. 25.
[3] W. Kurz and D.J. Fisher, *Fundamentals of Solidification* (Trans Tech Publications, Uetikon-Zürich, Switzerland, 1984), p. 13.
[4] K.A. Jackson and B. Chalmers, J. Appl. Phys. **29**, 1178 (1958).
[5] P. Mazur, in *Cryobiology*, edited by H.T. Meryman (Academic Press, London, 1966), p. 222.
[6] M. Toner and E.G. Cravalho, J. Appl. Phys. **67**, 1582 (1990).
[7] J.O.M. Karlsson, E.G. Cravalho, and M. Toner, Cryo-Lett. **14**, 323 (1993).
[8] K. Muldrew and L.E. McGann, Biophys. J. **66**, 532 (1994).
[9] J.P. Acker, J.A.W. Elliott, and L.E. McGann, Biophys. J. **81**, 1389 (2001).
[10] W.B. Hillig, J. Cryst. Growth **183**, 463 (1998).
[11] S.M. Alnaimi, J.H. Strange, and E.G. Smith, Magn. Reson. Imaging **12**, 257 (1994).
[12] R. Schmidt, E.W. Hansen, M. Stöcker, D. Akporiaye, and O.H. Ellestad, J. Am. Chem. Soc. **117**, 4049 (1995).
[13] K. Morishige and K. Kawano, J. Chem. Phys. **110**, 4867 (1999).
[14] J.S. Wettlaufer, Philos. Trans. R. Soc. London, Ser. A **357**, 3403 (1999).
[15] P. Mazur, Science **168**, 939 (1970).
[16] B. Rubinsky and D.E. Pegg, J. R. Soc. Lond. **234**, 343 (1988).
[17] K. Muldrew *et al.*, Cryobiology **40**, 102 (2000).
[18] Z. Liu, R. Wan, J.A.W. Elliott, S. Liang, and K. Muldrew, Cryobiology **41**, 367 (2000).
[19] K.R. Diller, Cryobiology **34**, 304 (1997).
[20] B. Rubinsky and M. Ikeda, Cryobiology **22**, 55 (1985).
[21] R.A. Alberty and R.J. Silbey, *Physical Chemistry* (Wiley, New York, 1992), p. 214.
[22] J.D. Cutnell and K.W. Johnson, *Physics*, 3rd ed. (Wiley, Toronto, 1995), p. 817.
[23] C.A. Ward and M.R. Sasges, J. Chem. Phys. **109**, 3651 (1998).
[24] J.W. Gibbs, Trans. Conn. Acad. Arts Sci. **III**, 108 (1875); republished in *The Scientific Papers of J. Willard Gibbs* (Dover Publications, New York, 1961), Vol. 1, p. 55.
[25] J.A.W. Elliott, Chem. Eng. Edu. **35**, 274 (2001).
[26] B. Chalmers, *Principles of Solidification* (Wiley, New York, 1964), p. 78.
[27] N.H. Fletcher, *The Physics of Rain Clouds* (Cambridge University Press, Cambridge, 1962), p. 205.
[28] L.R. Fisher and J.N. Israelachvili, Nature (London) **277**, 548 (1979).
[29] K. Koga, X.C. Zeng, and H. Tanaka, Phys. Rev. Lett. **79**, 5262 (1997).
[30] J.A. Sethian, *Level Set Methods and Fast Marching Methods* (Cambridge University Press, New York, 1996), p. 70.